FEATURE ARTICLE

Insights into the Structure and Function of Redox-Active Tyrosines from Model Compounds

Bridgette A. Barry*,† and Ólöf Einarsdóttir‡

School of Chemistry and Biochemistry, and the Petit Institute for Bioengineering and Bioscience, Georgia Institute of Technology, Atlanta, Georgia 30332, and Department of Chemistry and Biochemistry, University of California, Santa Cruz, California 95064

Received: November 17, 2004; In Final Form: January 14, 2005

Redox-active tyrosine residues play important roles in long distance electron-transfer reactions in enzymes, including prostaglandin H synthase, ribonucleotide reductase, and photosystem II. In cytochrome *c* oxidase, a cross-linked tyrosine−histidine cofactor has been proposed to play a role in proton and electron transfer reactions. Studies of tyrosyl radicals in model compounds, generated by UV photolysis, have recently provided new information about the structure and function of these redox-active species. The results of these studies, which combine magnetic resonance and optical spectroscopies, are described in this review.

Tyrosyl radicals are postulated to mediate catalysis in a number of enzymes, including prostaglandin H synthase,[1] ribonucleotide reductase (RNR),[2] and photosystem II (PSII).[3] Oxidation of tyrosine or tyrosinate results in the production of a neutral tyrosyl radical, which can then accept an electron to act as an intermediate in long distance electron transfer. The environmental factors responsible for functional control of these redox-active species have not as yet been elucidated. According to Marcus theory, the midpoint potential of the redox-active tyrosine influences the rate of biological electron transfer.[4] Possible influences over the midpoint potential include protein polarity, protein sequence, differential hydrogen bonding to the radical and the unphotolyzed state, and the nature of the coupled proton transfer reactions involving the radical. Another way of influencing the tyrosine redox function is through covalent bonding of another amino acid side chain to the tyrosine or tyrosinate ring to create a novel cofactor with potentially unique reactivity. Examples of such covalent modification are the cross-linked tyrosine−histidine cofactor in cytochrome *c* oxidase[5,6] and the cross-linked tyrosine−cysteine cofactor in galactose oxidase.[7]

Optical and magnetic resonance spectroscopies have been used to study the structure of tyrosyl and phenoxyl radicals in a variety of model compounds. In such model compounds, the radicals can be generated by ultraviolet photolysis.[8] Here, we discuss recent progress in understanding the structure and function of tyrosyl radicals and the cross-linked tyrosyl-histidine cofactor in cytochrome *c* oxidase.

Tyrosyl Radicals in Peptides: Delocalization of Electron Spin Density into the Peptide Bond?

Photolysis of tyrosine by UV light (266 nm) causes the loss of an electron from the aromatic ring. The electron is transferred to the solvent. The lifetime of the photolysis-induced radical has been reported to be 77 μs in aqueous solutions at room temperature and at pH 10.[9] The radical has a unique absorption band with a maximum at 400 nm.[10] Oxidation of the aromatic ring lowers the pK_A of the phenolic oxygen and leads to deprotonation of the ring.[11] At low temperature (77 K), the tyrosyl radical is stable.[8] The midpoint potential for tyrosine is pH dependent,[12,13] and a standard reduction potential of 0.9 V (vs SHE) has been reported at pH 7.0.

EPR studies of the tyrosyl radical indicate that the spin density is located on carbons 1, 3, 5 and on the phenolic oxygen (Figure 1A).[8,14−19] The EPR line shape is dependent on the details of this spin density distribution and on the dihedral angle (θ) at the $C_\beta-C_1$ bond. Previous EPR studies have shown that the total spin density on the aromatic ring and phenolic oxygen is close to one.[17,20] Raman vibrational studies have demonstrated that formation of the radical is also associated with perturbation of ring stretching vibrations and with a $\sim$300 cm^{-1} increase in the CO stretching frequency.[21−24] This increase in CO frequency has been attributed to delocalization of spin density onto the phenolic oxygen.[21]

In enzymes, redox-active tyrosines have different midpoint potentials and different electron-transfer rates. For example, PSII contains two redox-active tyrosine residues, D and Z, with different roles in PSII function and different physiochemical properties.[3,25] The two tyrosines have distinct midpoint potentials and decay kinetics that differ by many orders of magnitude (reviewed in ref 26). In RNR, the tyrosyl radical has been estimated to have a midpoint potential of $\sim$1 V (vs SHE)[27] and has been proposed to participate in long-range proton and electron-transfer events.[28,29] The focus of our recent work is modeling the effect of the protein environment on tyrosyl radical structure and function. Our experiments on model tyrosine-containing peptides have led to the hypothesis that spin density may delocalize into the peptide bond in these systems. Such delocalization could provide a mechanism by which both the

* Corresponding author.
† Georgia Institute of Technology.
‡ University of California, Santa Cruz.

10.1021/jp044749y CCC: $30.25
Published on Web 03/26/2005

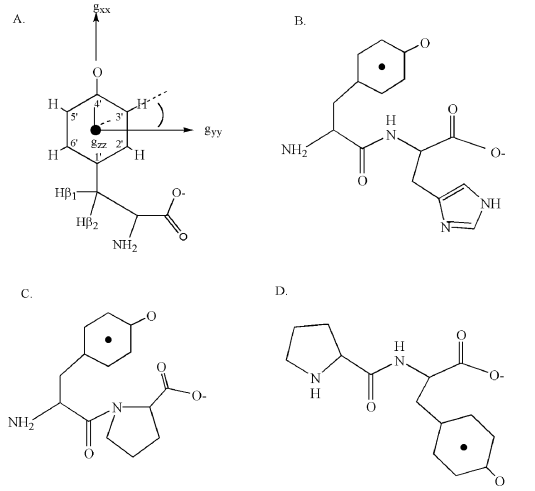

Figure 1. Structures and numbering of the tyrosyl radical (A). Structures of the Tyr−His (B), Tyr−Pro (C), and Pro−Tyr (D) dipeptides. The axis system in (A) shows the orientation of the *g* axis. Reproduced with permission from ref 33. Copyright (2002) American Chemical Society.

midpoint potential and electron-transfer rate are controlled by sequence and intramolecular interactions in tyrosyl radical-containing enzymes.

Peptides can sample multiple conformational states; the details of this conformational distribution are dependent on sequence.[30,31] The amide or, in the case of proline, imide bond is polar, and redistribution of electrons leads to a partial positive charge on the amide nitrogen and a partial negative charge on the carbonyl oxygen. This suggests an interaction between the electron-deficient π system of a tyrosyl radical and the amide bond.[32] To test this idea, we conducted experiments both on tyrosinate (Figure 1A) and on peptide models (see examples in Figure 1B−D). The results are summarized below.

EPR Spectra. EPR experiments demonstrate that tyrosyl radicals can be generated in dipeptides (Figure 1B−D) by UV photolysis at pH 11 (Figure 2). The line shape and *g* value of the radical observed after photolysis of tyrosinate at 77 K is typical of the aromatic tyrosyl radical (Figure 2A).[8] Labeling of the $C_{4'}$ aromatic carbon with ^{13}C has the expected effect of broadening the EPR spectrum (Figure 2B), and both the natural abundance and $^{13}C(1)$ spectra can be simulated (Figure 2A,B, dashed lines) with parameters typical of tyrosyl radical powder spectra.[9,33] In most of the dipeptides examined, including His−Tyr and Tyr−Ile (Figure 2C,D), photolysis produces a tyrosyl radical with an identical EPR line shape. However, in the Tyr−Pro dipeptide (Figure 2E), the EPR line shape is distinct. This difference can be simulated (Figure 2E, dashed line) with a 9° rotation at the $C_1'-C_\beta$ single bond.[33] The alteration in line shape is attributed to the imide bond to Pro, which introduces steric limitations on the conformation of the dipeptide. This experiment demonstrates the feasibility of using peptide models to study tyrosyl radical structure and function.

FT-IR Spectra. Vibrational spectroscopy was used to investigate the structure of the radical in more detail. In Figure 3, the FT-IR spectra of tyrosinate (Figure 3A) and $^{13}C(1)$ tyrosinate (Figure 3B) are presented. The single ^{13}C substitution will identify vibrational modes that involve motion of that carbon. These isotope-sensitive modes will include the symmetric ring stretching (υ_{8a}, υ_{19a}) and the CO stretching ($\upsilon_{7a'}$) vibrations of the molecule. In agreement with previous reports, isotope-sensitive modes at 1602 (υ_{8a}), 1500 (υ_{19a}), and 1266 ($\upsilon_{7a'}$) cm^{-1} are observed in Figure 3B. In the FT-IR spectra of

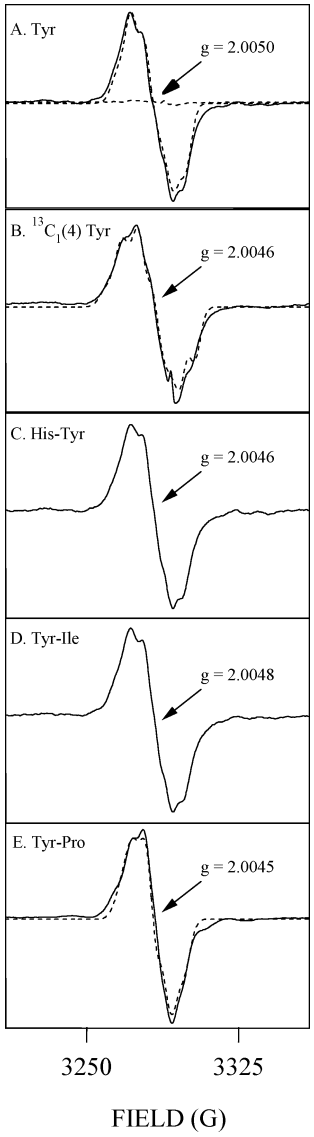

Figure 2. EPR spectra of tyrosyl radicals generated by UV photolysis of solutions containing (A) tyrosinate (solid line), (B) $^{13}C(1)$ tyrosinate (solid line), (C) His−Tyr, (D) Tyr−Ile, and (E) Tyr−Pro (solid line). Simulations of the EPR spectra are shown as dashed lines in A, B, and E. (A, dotted line) shows the result of UV photolysis of the borate buffer. Reproduced with permission from ref 33. Copyright (2002) American Chemical Society.

the dipeptides,[9,33] bands with similar frequencies were observed (data no shown). For example, the frequency range for υ_{8a} was 1602−1600 cm^{-1} and 1269−1266 cm^{-1} for $\upsilon_{7a'}$. Potential assignments of the other FT-IR bands have been discussed.[33]

FT-IR Photolysis Spectra: Tyrosinate. FT-IR difference spectroscopy was used to identify the changes in electronic structure that accompany the photolysis reaction. Spectra were recorded before and after photolysis and subtracted to generate a difference spectrum. Figure 4 presents photolysis-induced difference spectra acquired from tyrosinate (Figure 4B), $^{13}C(1)$ tyrosinate (Figure 4C), and ^{15}N tyrosinate (Figure 4D) at 77 K and pH 11. As observed in Figure 4A, photolysis of the borate buffer alone gives no vibrational bands. However, photolysis of tyrosinate (Figure 4B) gives a well-defined difference spectrum, showing the effect of radical formation on the vibrational bands. Negative bands are unique vibrational modes of the unphotolyzed state; positive bands are unique vibrational modes of the radical. Among the negative bands are three vibrational bands attributed in the discussion above to υ_{8a}, υ_{19a},

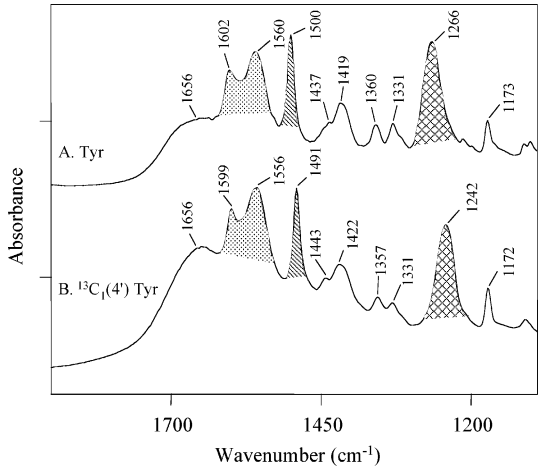

Figure 3. FT-IR spectra of (A) tyrosinate and (B) ^{13}C(1) tyrosinate. Spectral contributions from the borate buffer were subtracted from these data. The tick marks on the *y*-axis represent 0.4 absorbance units. Crosshatched lines are assigned to ring modes and the CO stretching vibrations of tyrosinate. Reproduced with permission from ref 33. Copyright (2002) American Chemical Society.

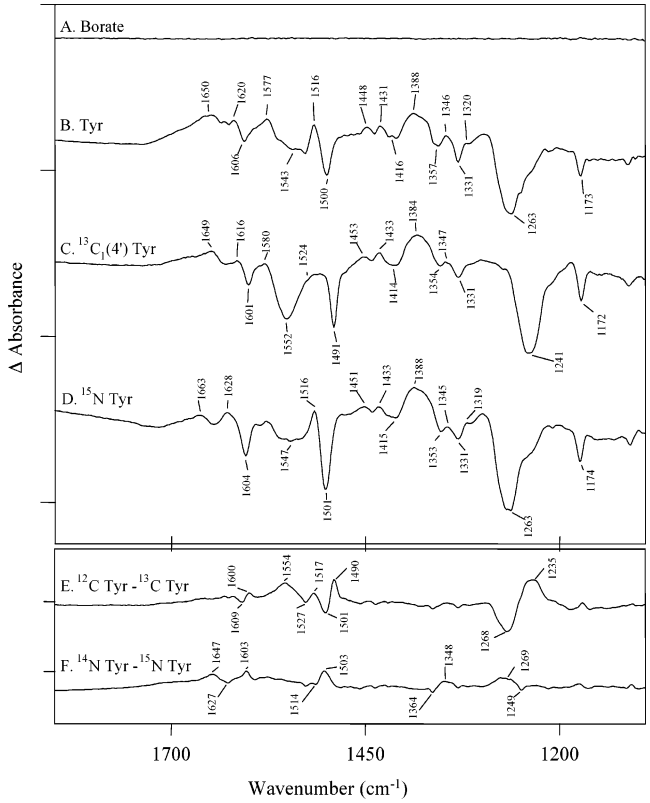

Figure 4. Difference FT-IR spectra, associated with UV photolysis, of (A) 10 mM borate buffer pH 11, (B) tyrosyl radical-minus-tyrosinate, (C) ^{13}C(1) tyrosyl-minus-^{13}C(1) tyrosinate, and (D) ^{15}N tyrosyl-minus-^{15}N tyrosinate. Data obtained before UV illumination were subtracted from data collected after illumination to generate these difference spectra. In (E), the double difference spectrum, ^{12}C (B)-minus-^{13}C (C), is shown. In (F), the double difference spectrum, ^{14}N (B)-minus-^{15}N (D), is shown. Tick marks on the *y*-axis represent 0.02 AU. Reproduced with permission from ref 33. Copyright (2002) American Chemical Society.

and $\upsilon_{7a'}$. These three bands exhibit the expected isotope sensitivity when ^{13}C is substituted at the $C_{4'}$ carbon (compare Figure 4B and 4C). This is especially apparent in the isotope-edited, double difference spectrum (Figure 4E) in which the 1609 cm^{-1} band is observed to shift to 1600 cm^{-1}, the 1501 cm^{-1} band shifts to 1490 cm^{-1}, and the 1268 cm^{-1} band shifts to 1235 cm^{-1}. Isotope-sensitive positive bands attributable to υ_{8a} and $\upsilon_{7a'}$ of the radical are also observed in Figure 4B. In the isotope-edited spectrum (Figure 4E), these bands contribute at 1554 and 1517 cm^{-1}, but the locations of their isotope-shifted lines are not apparent. Based on previous work, the large increase in the frequency of the CO stretching vibration, when the radical and the unphotolyzed molecule are compared, is expected and consistent with radical formation.[21−24]

^{15}N labeling of tyrosinate was also employed in the FT-IR photolysis studies (Figure 4D) and ^{15}N isotope bands were identified (Figure 4F). This result suggests an interaction between the unpaired spin, localized mainly on the aromatic ring, and the amino nitrogen. For example, in the ^{15}N isotope-edited spectrum (Figure 4F), ^{15}N sensitive bands at 1647/1627/1603 cm^{-1} are identified. Density functional calculations support the assignment of a band at ∼1627 cm^{-1} to an NH deformation mode in tyrosinate and suggest that delocalization of spin to the amino nitrogen would increase the frequency of this vibration in the radical (unpublished results, K. Range, I. Pujols-Ayala, B. A. Barry and D. York). Density functional calculations were also employed to quantitatively predict the spin density distribution.[33] In the Boltzmann weighted average, the amount of spin density on the amino N was predicted to be 0.02 and to be conformation dependent.[33] This amount of spin density is consistent with a hyperfine coupling to nitrogen in the tyrosyl radical, but the magnitude of the coupling is predicted to be small (0.4 G) and therefore the coupling is not expected to be detectable in field-swept EPR studies.[33] Spin density may delocalize from the aromatic system to the amino group because of a through-space, spin polarization mechanism. Such a mechanism has been proposed to be relevant to electronic structure in tryptophan cation radicals.[32]

FT-IR Photolysis Spectra: Tyrosine-Containing Dipeptides. If there is an electronic interaction between the aromatic ring and the amino group in the tyrosyl radical, then one would expect an interaction between the aromatic group and the amide (or imide) bond in tyrosyl radical-containing dipeptides. The advantage of dipeptides over more complex peptides is that dipeptides contain only one peptide bond and there is no possibility of transition dipole coupling, which complicates interpretation.[34] For methylacetamide, the amide I band (CO s, 83%) is calculated to absorb at 1646 cm^{-1}; the amide II band (NH ib 49%; CN s 33%) is calculated to occur at 1515 cm^{-1}.[34] In peptides, the amide I is often observed at lower frequencies (∼1630 cm^{-1}) compared to proteins, due to extensive hydrogen bonding with solvent.[35,36]

In Figure 5, FT-IR difference spectra following UV photolysis were acquired from tyrosine-containing dipeptides. Bands from the tyrosine and tyrosyl radical states are observed. In dipeptides with the sequence, X−Tyr, derivative shaped bands between 1554 and 1531 cm^{-1} are observed (Figure 5E−H). These bands are attributable to an amide II vibrational band. A negative band between 1628 and 1621 cm^{-1} is also observed in these dipeptides and is attributable to an amide I vibrational band. In Tyr−X dipeptides (Figure 5A−D), these bands are not as evident, except in the Tyr−Ile and Tyr−Pro dipeptides (Figure 5B,C). These data support the interpretation that a spin interaction can occur between the aromatic ring and the amide or imide bond in the X−Tyr peptides. Also, note that small sequence-dependent changes are observed in the frequency of tyrosine and tyrosyl radical bands in Figure 5. In recent work, we have also detected amide I bands in the photolysis spectrum of tyrosine-containing pentapeptides (data not shown).

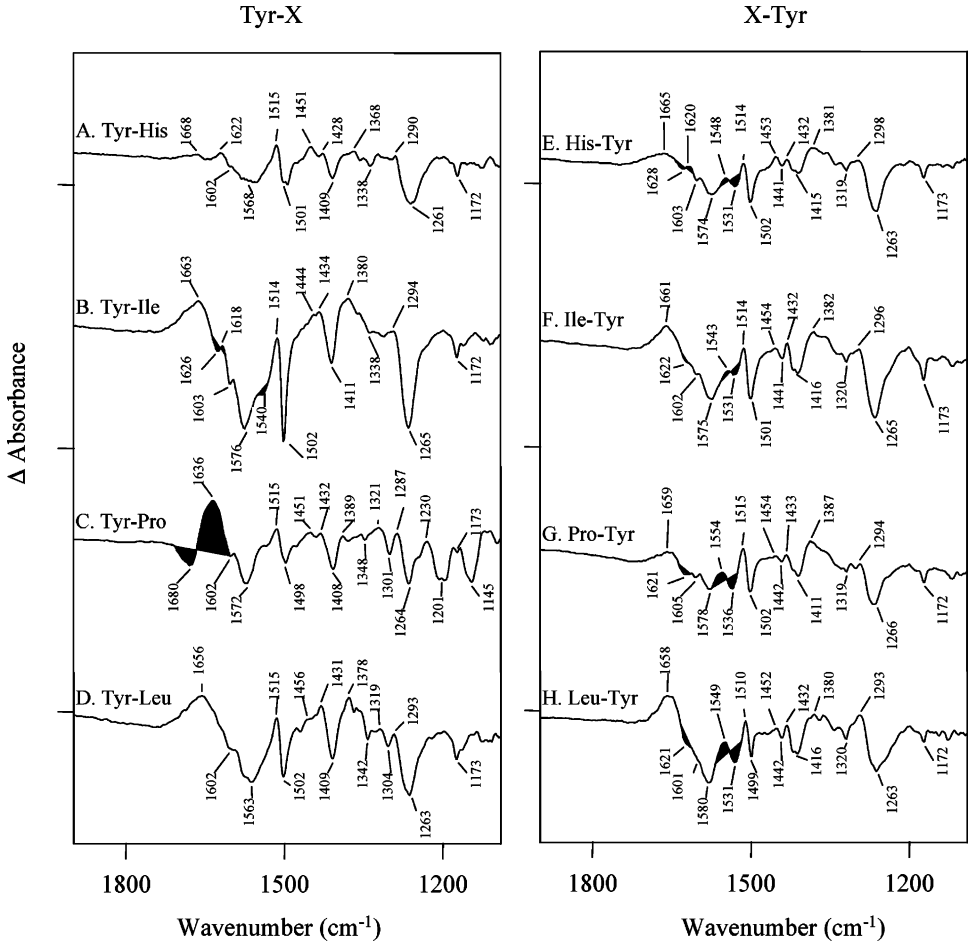

Figure 5. Difference FT-IR spectra, associated with UV photolysis, of (A) tyrosyl−histidine-minus-tyrosinate−histidine, (B) tyrosyl−isoleucine-minus-tyrosinate−isoleucine, (C) tyrosyl−proline-minus- tyrosinate−proline, (D) tyrosyl−leucine-minus-tyrosinate−leucine, (E) histidine−tyrosyl-minus-histidine−tyrosinate, (F) isoleucine−tyrosyl-minus- isoleucine−tyrosinate, (G) proline−tyrosyl-minus-proline−tyrosinate, and (H) leucine−tyrosyl-minus-leucine−tyrosinate. Data obtained before UV illumination were subtracted from data collected after illumination to generate these difference spectra. Tick marks on the *y*-axis represent 0.04 AU. Bands assigned to amide I, amide II, and proline vibrational modes have solid fill. Reproduced with permission from ref 33. Copyright (2002) American Chemical Society.

Summary and Perspectives. There are two ramifications of the spin density delocalization that should be emphasized here. The first is that such a delocalization mechanism provides a means for controlling the midpoint potential in tyrosyl radicals. Because the delocalization will lower the energy of the radical state but not the unphotolyzed state, the degree of spin delocalization can alter the reduction potential of the redox-active amino acid. This trend can be observed in a comparison of the reduction potentials of phenol and substituted phenol derivatives, such as *p*-cresol and *p*-methoxyphenol.[12] The second is that such a delocalization mechanism provides a method for directional control. If the direction of delocalization is sequence dependent, then the rate of electron transfer, which is exponentially dependent on distance,[4] can be controlled by selective delocalization of unpaired spin into one of the two amide bonds near the redox-active center. In future work, these ideas will be tested and explored.

Cross-Linked, Redox-Active Tyrosine Residue in Cytochrome *c* Oxidase?

Modified tyrosine residues may also play an important role in biological processes and have been shown to be present at the active sites of several enzymes.[37] This includes the copper enzyme, galactose oxidase,[38,39] copper-dependent amine oxidases, methylamine dehydrogenase, catalase (for review, see ref 37), and most recently, heme−copper oxidases,[39,40] which will be our focus. The heme−copper oxidases join a growing list of proteins that contain post-translationally modified redox-active amino acids.[37,41]

Heme−copper oxidases play crucial roles in energy transduction mechanisms by catalyzing the reduction of dioxygen to water (Scheme 1) in eukaryotes and in many aerobic bacteria.[42−45] This reaction is coupled to the translocation of four protons across the mitochondrial or plasma membrane.[46] The resulting electrochemical proton gradient is used to drive ATP synthesis, which is catalyzed by ATP synthase. In addition to the translocated protons, four scalar protons are required for the formation of two water molecules from dioxygen. Proton uptake takes place through two channels, the D-pathway and the K-pathway, which have been identified from the enzyme's crystal structure.[5,6,47,48] The D-pathway is believed to be responsible for the uptake of the scalar and translocated protons during the oxidation of the enzyme by dioxygen,[49−54] while proton uptake during the reduction of the oxidized enzyme has been associated with the K-pathway.[49,55−60]

The reduction of dioxygen to water takes place at the binuclear center, which comprises heme a_3 and Cu_B. The low-spin heme *a* and the dinuclear Cu_A center constitute the other two redox centers. In addition, the X-ray crystal structures of the bovine heart oxidase[6] and the *Paracoccus denitrificans* enzyme[5] have revealed that the C6 of tyrosine 244 (bovine heart numbering), located at the end of the K-channel proton-transfer

SCHEME 1: Schematic Illustration of the Reaction of Fully Reduced Cytochrome Oxidase (R) with Dioxygen (adapted from Refs 62 and 73 and Modified)[a]

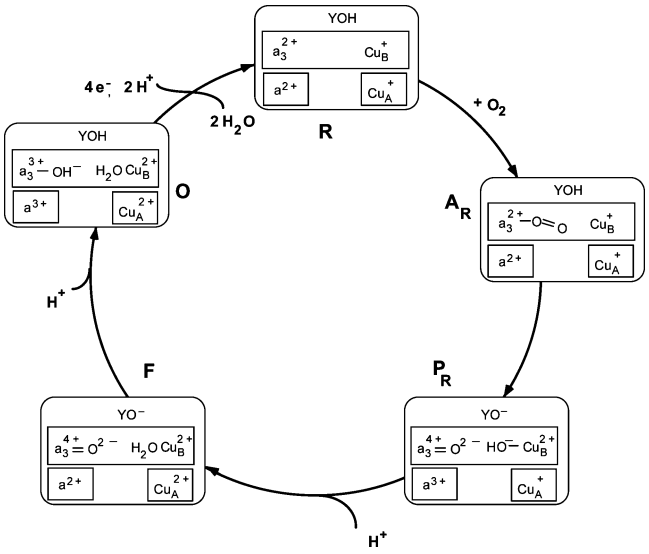

[a] The YOH represents the cross-linked tyrosine. In the fully reduced enzyme, heme *a* donates an electron to the binuclear center in compound **A** (**A**$_{\mathbf{R}}$), generating the so-called **P**$_{\mathbf{R}}$ intermediate, followed by proton uptake from the solution forming the **F** state. In the final step, an electron from the equilibrated heme *a*/Cu$_A$ is transferred to the binuclear center generating the oxidized state. Addition of four electrons to the oxidized state generates the fully reduced enzyme. The structure of the **P**$_{\mathbf{R}}$ intermediate has not been experimentally verified.

pathway, is cross-linked to the ϵ-nitrogen of histidine 240, a ligand to Cu$_B$. The presence of the cross-link has more recently been observed in the X-ray structure of the *Thermus thermophilus* cytochrome *c* oxidase;[61] however, the X-ray structure of the *Rhodobacter sphairoides* enzyme was inconclusive regarding the presence of the cross-link.[62] The cross-link is most likely the result of a post-translational modification and does not arise from X-ray treatment of the crystals as shown by protein chemical analysis.[63] The post-translational modification has been reported to be essential for the catalytic activity of the enzyme and for maintaining a functional environment of the binuclear center.[64] Other studies have suggested that the heme a_3 site is intact but the coordination environment of Cu$_B$ is altered when the tyrosine is mutated.[65]

The reduction of dioxygen to water requires four electrons (Scheme 1), two of which come from the oxidation of heme a_3 (Fe^{2+} to Fe^{4+}) and one from the oxidation of Cu_B^+ to Cu_B^{2+}. In the reaction of dioxygen with the mixed-valence enzyme, in which heme a_3 and Cu$_B$ are reduced and heme *a* and Cu$_A$ oxidized, the cross-linked tyrosine has been proposed to provide the fourth electron and a proton required for the cleavage of the dioxygen bond, thus generating a neutral tyrosyl radical in the **P**$_{\mathbf{M}}$ intermediate of the enzyme[66] (Scheme 2). In the reaction of the fully reduced enzyme with dioxygen, heme *a* is proposed to provide the reducing equivalent for breaking the dioxygen bond (Scheme 1).

Iodide labeling and protein peptide analysis suggest that a tyrosyl radical is formed during the O−O bond cleavage, generating the **P**$_{\mathbf{M}}$ intermediate,[67] but theoretical studies on models of the binuclear center indicate that the barrier for simultaneous transfer of an electron and a proton is high and that the tyrosine may only provide the electron required for the cleavage of the oxygen bond.[68] An alternative hypothesis is that in the early stage of the O−O bond cleavage, the electron is donated by another residue, possibly tryptophan 236, an amino

SCHEME 2: Proposed Mechanism for the Reaction of the Mixed-valence Cytochrome Oxidase with Dioxygen[a]

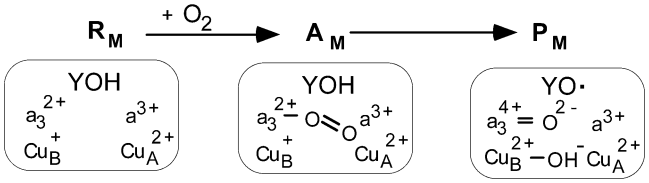

[a] The YOH represents the cross-linked tyrosine. The cross-linked tyrosyl radical in **P**$_{\mathbf{M}}$ has not been experimentally verified.

acid close to the binuclear center and conserved in all heme−copper oxidases, with subsequent radical transfer to the cross-linked tyrosine.[68,69] However, the expected EPR signals from the Cu_B^{2+} and the tyrosyl radical (Scheme 2) have not been detected in the EPR spectrum of the **P**$_{\mathbf{M}}$ form of the enzyme. Babcock and co-workers have proposed that the lack of the EPR signals may stem from spin coupling between the unpaired electron on Cu$_B$ ($S = 1/2$) and the tyrosyl radical ($S = 1/2$).[66] Although results from several groups are consistent with a possible role of a tyrosyl radical in dioxygen reduction,[66,67,70−74] direct evidence has been lacking.

Spectrophotometric Titrations. One of the key questions regarding the role of the cross-linked tyrosine in the mechanism of the reduction of dioxygen to water centers on its possible function as a proton donor during dioxygen bond cleavage. If the cross-linked tyrosine does indeed act as a proton donor, one would expect a lowering of the pK_a of the phenolic proton compared to that of unperturbed phenol or tyrosine. To answer this question, we recently synthesized and characterized by spectroscopic techniques a chemical analogue of the His−Tyr cross-link and the radical generated upon UV-photolysis of the compound.[9] The synthesis of the His-phenol cross-linked complex is based on the coupling of the imidazole with arylleadtriacetate in the presence of catalytic amounts of Cu(OAc)$_2$.[9,75] The reaction uses stoichiometric amounts of both coupling partners and proceeds at room temperature in a few hours without the addition of base and without racemization.

The pK_a of the cross-linked compound and that of tyrosine and *p*-cresol were determined from the absorption spectra recorded over a wide pH range.[9] Singular value decomposition and global p*K* fitting resulted in two pK_a values of 5.54 and 8.34, assigned to the ϵ-nitrogen of the imidazole and the phenolic proton, respectively (Figure 6). The pK_a of the phenolic proton is considerably lower than that obtained for tyrosine (10.2) and *p*-cresol (10.2). The values are similar to those reported by McCauley et al. for the cross-linked model compound, 2-imidazol-1-yl-4-methyl-phenyl.[76] The slightly different values reported by Collman and co-workers[77] for other model compounds may be due to substituent effects.[40] The lower phenolic pK_a observed in the cross-linked model compounds is consistent with recent hybrid density functional therory calculation on the effect of a variety of ortho-substituents, including imidazole, on the acidity of phenol.[78] McCauley et al.[76] also reported an increase in the oxidation potential of 2-imidazol-1-yl-4-methyl-phenyl of 66 mV compared to that of *p*-cresol. Together these results suggest that the change in electronic structure arising from the histidine-tyrosine cross-link may indeed facilitate proton delivery to the active site in the heme−copper oxidases. This may occur either through an inductive electron-withdrawing effect polarizing the O−H bond or by delocalization of the negative charge by the cross-linked imidazole, thus stabilizing the anion.[76,78]

Evidence for Radicals in Heme−Copper Oxidases? Another question concerns the nature of the cross-linked tyrosyl

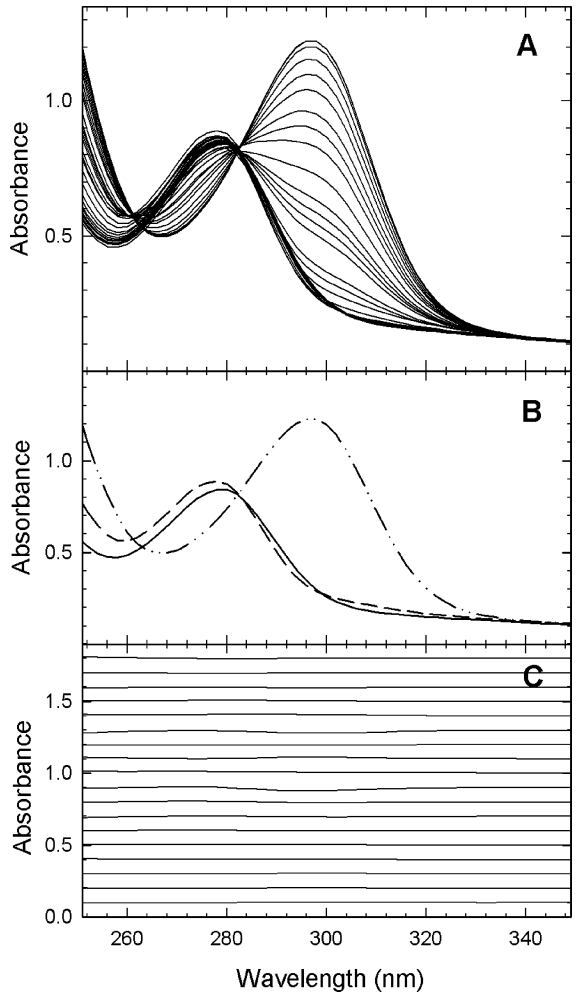

Figure 6. (Panel A) Spectrophotometric titration of an aqueous solution of the His−phenol cross-linked compound (1.0 mM) from pH 2.5 to 10.63. The data were analyzed using SVD and global pK_a fitting, which provided the spectral forms of the different protonation states of the His−phenol compound (panel B). The residuals show the difference between the fit and the data using pK_as of 5.54 and 8.34 (panel C). Reproduced with permission from ref 9. Copyright (2002) American Chemical Society.

radical in cytochrome oxidase, if present, and more specifically, the possible spin coupling between the unpaired electron on Cu_B and the tyrosyl radical with possible delocalization of spin density onto the imidazole. Different amino acid radicals have been reported to be formed when the **P** compound is generated upon addition of hydrogen peroxide to the oxidized enzyme.[71,74,79,80] A broad EPR signal in the **P** form of the bovine enzyme was attributed to a tryptophan radical,[80] while in the *Paracoccus* enzyme a similar broad EPR signal, but with a resolved hyperfine structure, was proposed to originate from a tyrosyl radical, possibly the cross-linked tyrosine.[71] Recent studies aimed at reconciling the differences between the two studies have simulated the EPR spectra as arising from Tyr129 (bovine heart numbering), which is conserved among the different oxidases but is ∼10 Å from the binuclear center.[81] A primary radical formation at the His−Tyr cross-link was proposed, with subsequent transfer of the radical to Tyr129. MacMillan and coworkers have recently suggested that the radical species observed in the reaction of the *Paracoccus denitrificans* cytochrome c oxidase with hydrogen peroxide is from Tyr 129 (Tyr 167 in *P. denitrificans*).[98] Electron spin resonance trapping experiments using 2-methyl-2-nitrosopropane (MNP) are consistent with a tyrosyl radical being formed

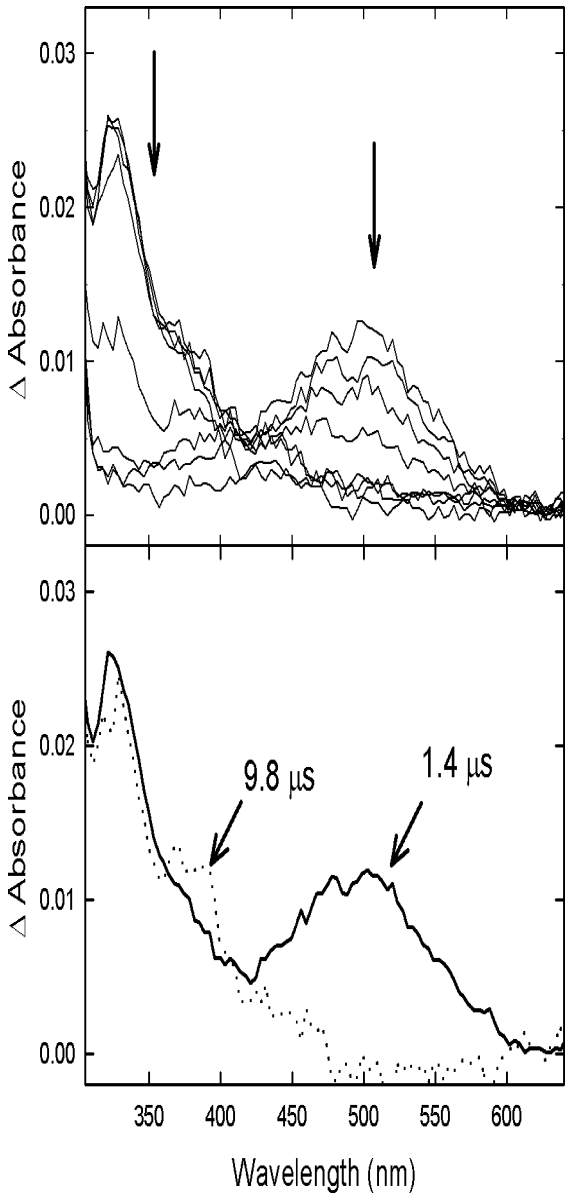

Figure 7. (Top) Time-resolved difference spectra (post- minus pre-photolysis) of aqueous solutions of the His-phenol cross-linked compound (1.78 mM) following excitation at 266 nm (Nd:YAG, 4th harmonic 7 ns pulse) at room temperature. The laser power was 300 mJ/mm^2. The probe beam was a xenon flash lamp, and the signals were detected by an optical multichannel analyzer using a 100 μm slit and 200 ns gate. The buffer was 0.1 M $NaHCO_3$/0.06 M *tert*-butyl alcohol (pH 10), and the samples were purged with N_2O just prior to use (to remove absorption contribution from the solvated electron). (Bottom) The intermediate spectra of the His−phenol complex resulting from the SVD/global exponential fitting and using a unidirectional sequential mechanism. The apparent lifetimes were 1.4 and 9.8 μs. Reproduced with permission from ref 9. Copyright (2002) American Chemical Society.

upon addition of hydrogen peroxide to the bovine heart enzyme.[82]

Time-Resolved Optical Absorption Spectroscopy. We have used time-resolved optical absorption spectroscopy at room temperature to explore the nature of the radical generated upon exciting the His−phenol model complex at 266 nm.[9] The time-resolved optical absorption difference spectra of the UV-generated radical indicated an intermediate with absorption maxima at ∼500 and ∼325 nm and a lifetime of ∼1 μs (Figure 7). We attributed this species to a phenoxyl radical species. The peak maximum at 500 nm is significantly red-shifted relative

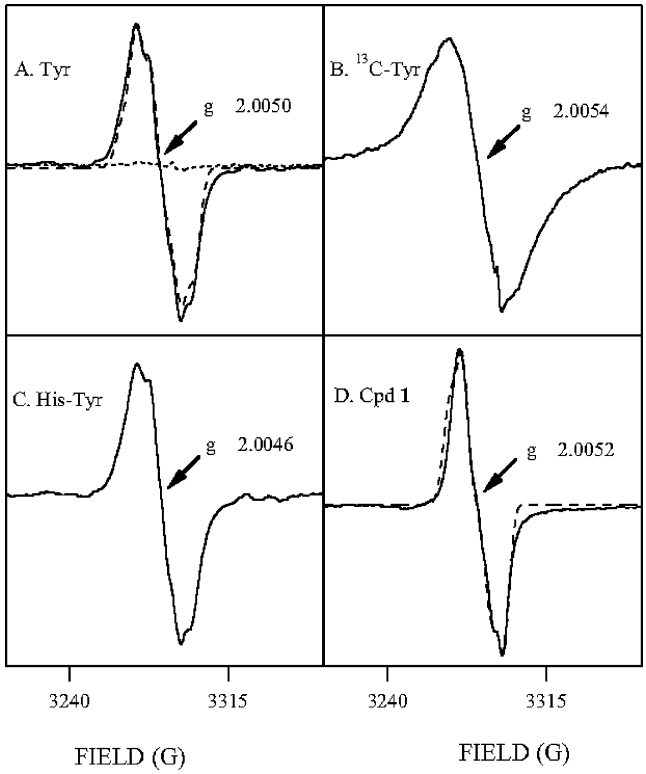

Figure 8. EPR spectra of free radicals produced in solutions of tyrosine (A, solid line), ^{13}C(6)−tyrosine (B), His−Tyr dipeptide (C), and His−phenol cross-linked compound (Cpd 1) (D, solid line). Samples were 100 mM and also contained 10 mM borate−NaOH, pH 11. The radicals were generated by UV photolysis at 77 K. EPR simulations are superimposed as the dashed line in (A) and (D). The dotted line in (A) is a negative control showing the results obtained with borate buffer alone. Reproduced with permission from ref 9. Copyright (2002) American Chemical Society.

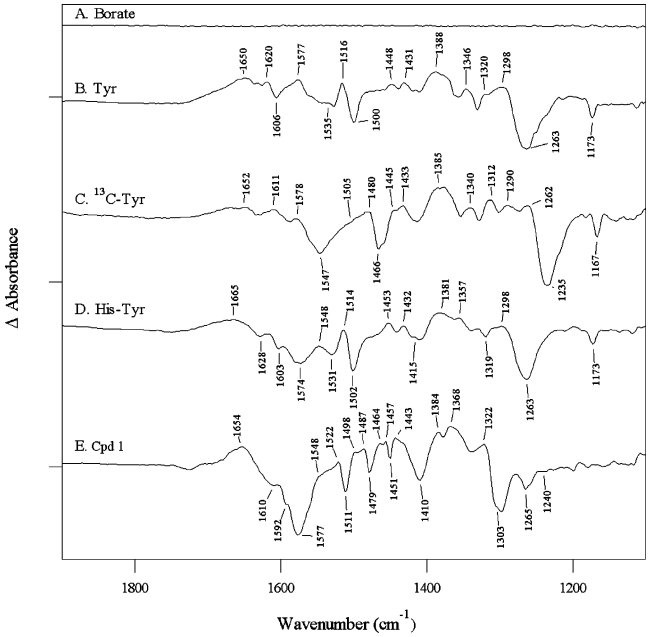

Figure 9. Difference FT-IR spectra associated with the production of radicals by UV photolysis at 77 K. The samples were borate alone (A), tyrosine (B), ^{13}C(6)−tyrosine (C), His−Tyr dipeptide (D), and His−phenol cross-linked compound (Cpd 1) (E). Individual difference spectra correspond to a total of 4 min of data acquisition, 2 min before UV photolysis and 2 min after photolysis. The difference spectra were constructed by directly ratioing data obtained after 5 (A−D) or 10 (E) laser flashes to data obtained before photolysis. To obtain the final signal-to-noise ratio, spectra were averaged over eight (A), two (B) or three (C−D) different samples. Tick marks on the *y*-axis represent 2 $\times$ 10^{-2} AU. Reproduced with permission from ref 9. Copyright (2002) American Chemical Society.

to the 400 nm absorption maximum observed for an unperturbed phenoxyl radical.[9] This could be due to more extensive conjugation in the former or significant mixing of the imidazole and phenoxyl electronic states in the cross-linked compound.[10,21]

EPR Spectra. To further explore the possible delocalization of the spin density of the cross-linked radical onto the imidazole, we recorded a low-temperature EPR spectrum of the UV-irradiated His-phenol cross-linked compound.[9] The spectrum confirmed the presence of a radical. Figure 8 (solid lines) shows a comparison of the EPR spectra of the UV-generated radicals for tyrosine (A), ^{13}C(6) tyrosine, which is labeled at all six ring positions, (B), the His−Tyr dipeptide (C), and the His−phenol cross-linked compound (D). The difference in line shape between the spectra of the tyrosine and the cross-linked His-phenol arises from the lack of β-methylene protons in the latter. The g value of the His−phenol radical was 2.0052 $\pm$ 0.001, which was not significantly different from the g value for the unperturbed tyrosyl radical of 2.0050 $\pm$ 0001. This indicates similar spin density on the phenolic oxygen in the two species. This conclusion was supported by simulation of the respective spectra (Figure 8A and D, dashed lines), which indicated a small coupling to the imidazole nitrogen and little spin density perturbation in the phenoxyl ring. Recent calculations of Himo and co-workers have confirmed the lack of effect of the cross-link on the spin distribution and the g values of the tyrosyl radical.[83] Our results are also supported by recent density functional calculations (DFT) and simulations of EPR spectra of 4-methyl-2-(4-methyl-imidzole-1-yl) phenol, a model of the His−Tyr cross-link in the enzyme, which did not require hyperfine couplings to the nitrogen nuclei.[84] Interestingly, UV resonance Raman studies of *ortho*-imidazole-bound *para*-cresol model complex of the His−Tyr cross-link found that some of the imidazole vibrations were resonance enhanced upon excitation of the $\pi\pi^*$ transition of the phenol.[85] This was interpreted in terms of significant delocalization of the π-electrons between the imidazole and phenol rings via the covalent linkage.

Photolysis-Induced FT-IR Spectra of the Cross-Linked Compound and Comparison with Infrared Assignments in the Heme−Copper Oxidases.

His−Phenol Cross-Linked Compound. FT-IR difference spectroscopy is a powerful tool to probe structures of biological molecules and has provided valuable information about heme−copper oxidases (for review, see Gennis[86]). We have used FT-IR to investigate the differences between the structure of the radicals generated from tyrosine and our histidine−phenol cross-linked compound.[9] Figure 9 shows the photolysis-induced difference spectra (after minus before photolysis) for tyrosine (A), ^{13}C(6) tyrosine (B), the His−Tyr dipetide (C) and the His−phenol cross-linked compound (D) at pH 11. The positive bands represent vibrational modes unique to the tyrosine radical, while the negative bands arise from unique modes of the unphotolyzed tyrosinate. The positive bands at 1516 and 1514 cm^{-1} in the photolyzed difference spectra of tyrosine and the His−Tyr dipeptide, respectively, were attributed to the C−O stretch of the tyrosyl radical, in agreement with previous assignment of this band.[21−24,87] This assignment was supported by ^{13}C labeling, which shifted the band to 1480 cm^{-1}. However, there was no vibrational band at 1514−1516 cm^{-1} or at 1505 cm^{-1} in the photolysis spectrum of the His−phenol cross-linked compound.

Positive bands were observed at 1522, 1498, and 1487 cm^{-1}, and we tentatively assigned either the band at 1522 or 1498 cm^{-1} to the C−O stretching vibration of the cross-linked radical. The small shift in the band relative to the C−O vibration in the unperturbed tyrosine radical is consistent with the small hyperfine coupling used in the EPR simulation.

The P_M Intermediate: the C−O and C−C Stretching Vibrations. A band at 1489 cm^{-1} in the resonance Raman spectrum of the $\mathbf{P_M}$ intermediate (Scheme 2) of cytochrome bo_3 has been assigned to the C−O stretching mode of the cross-linked tyrosyl radial.[72] A band at 1479 cm^{-1} in the $\mathbf{P_M}$-minus-**O** IR and ATR-FTIR difference spectra of cytochrome oxidase from *Rhodobacter*[73] and bovine heart enzyme,[88] respectively, has tentatively been assigned to the same vibration. In the UV-resonance resonance Raman spectrum of the deprotonated neutral radical form of *ortho*-imidzole-bound *para*-cresol, a model compound for the cross-linked histidine−tyrosine, a band at 1530 cm^{-1} was attributed to the C−O stretching vibration of tyrosine 244.[85] Heberle and co-workers observed bands at 1528 and 1517 cm^{-1} in the $\mathbf{P_M}$-minus-**O** IR difference spectrum of the *Rhodobacter* oxidase and attributed either of the two bands to the C−C stretch of the cross-linked tyrosyl radical.[73] A positive band has been observed at ∼1520 cm^{-1} in the $\mathbf{P_M}$-minus-**O** difference spectrum of the bovine heart enzyme.[88,89] The good correlation between the vibrational signatures in the spectra of the $\mathbf{P_M}$ state of the enzyme[72,73,88,89] and those present in the spectra of the radical forms of the model compounds[9,85] provides strong support for the formation of a neutral tyrosyl radical in the $\mathbf{P_M}$ form of the enzyme.

The F and O Intermediates: The C−O and C−C Stretching Vibrations. If the cross-linked tyrosine can serve as a proton and electron donor during the breakage of the dioxygen bond, can it also serve as a proton donor during other steps in the catalytic cycle? Scheme 1 shows a proposed mechanism for the oxidation of fully reduced oxidase by dioxygen. As stated above, in the reaction, heme *a* is believed to provide the reducing equivalent for breaking the dioxygen bond, although a prior formation of a tyrosyl radical cannot be excluded.

Heberle and co-workers recently reported the infrared difference spectra of several functional intermediates of cytochrome oxidase, including **F**.[73] A negative band was observed at 1248 cm^{-1} in the **F**-minus-**O** infrared difference spectrum,[73] which was attributed to the C−O stretching of protonated tyrosine in the oxidized state of the enzyme. A negative band at the same frequency was observed in a tyrosinate-minus-tyrosine model compound, difference spectrum.[73] Hellwig and co-workers have assigned a signal at 1249 cm^{-1} to the C−O stretching mode of a protonated tyrosine;[90] for deprotonated tyrosine the C−O stretching mode was assigned at 1269 cm^{-1}. In our studies, we attributed a band at 1266 cm^{-1} to the C−O stretching mode of deprotonated tyrosine;[9] the shift of this band to 1238 cm^{-1} upon ^{13}C labeling is consistent with this assignment. In the FT-IR spectrum of our His−phenol complex (pH 11), a much less intense band was observed at 1265 cm^{-1}, with another band at 1241 cm^{-1}.[9]

Based on the comparisons above, the cross-linked tyrosine is expected to be deprotonated in the **F** intermediate of the enzyme and protonated in the oxidized form (Scheme 1).[73] This conclusion is supported by the observation of a negative 1515 cm^{-1} band in the **F**-minus-**O** infrared difference spectrum of the *Rhodobacter* enzyme.[73] This band was also present in the IR difference spectrum of deprotonated-minus-protonated tyrosine[73] and has been assigned to the phenyl ring stretching mode of protonated tyrosine.[73,91]

The Two-Electron and Fully Reduced Enzyme: The C−C Ring Stretching Vibrations. When cytochrome oxidase is prepared in the CO-bound form, a laser flash can be used to photodissociate CO from heme a_3. Difference FT-IR spectra, associated with the release of CO, can be constructed both for the fully reduced and the mixed valence enzyme. A positive 1515 cm^{-1} band in these difference spectra has been assigned to a ring stretching vibration of protonated tyrosine 244.[92] A positive band was observed at this frequency in the infrared spectrum of the protonated 2-(4-methyl-1*H*-imidazol-1-yl)-4-methylphenol model complex.[93]

Based on the results reviewed above, the cross-linked tyrosine appears to be protonated in the fully oxidized enzyme, a neutral radical in the $\mathbf{P_M}$ state, deprotonated in the **F** intermediate, and protonated in the two-electron-reduced and four electron-reduced enzyme. These studies indicate that the cross-linked tyrosine may play a significant role in the mechanism of reduction of dioxygen to water. The infrared studies have also provided crucial information regarding the protonation state of glutamate 242 (bovine heart numbering) in different functional intermediates of the enzyme.[73] This residue appears to play a key role in the proton-transfer reactions of the enzyme.[52]

Other Vibrational Modes of the Cross-Linked Compound and the Heme−Copper Oxidases. Infrared bands specific to the Tyr−His bi-ring structure have also been reported. Based on isotopic labeling and normal-mode analysis, bands at 1480 and 1546 cm^{-1} in the infrared spectra of a protonated model complex of the cross-linked tyrosine, 2-(4-methyl-1*H*-imidazole-1-yl)-4-methylphenol, were attributed to a coupled Tyr and His ring mode, with a significant contribution from the CN of the covalent linkage.[93] Based on this assignment, positive bands at ∼1480 and ∼1550 cm^{-1} in the FTIR difference spectra of the photolyzed bo_3−CO oxidase from *E. coli*,[93] and a negative band at 1546 cm^{-1} in the **F**-minus **O** difference spectrum of the *Rhodobacter* oxidase[73] have been assigned to the bi-ring structure. Negative bands have also been reported at 1546 and 1542 cm^{-1} in the $\mathbf{P_M}$-minus-**O** difference spectrum of the bovine enzyme and *Paracoccus denitrificans* enzymes, respectively, but not in the **F**-minus-**O** difference spectrum.[89] We observed a band at 1478 cm^{-1} in the FT-IR spectrum of the deprotonated His−phenol complex, which we tentatively assigned to vibration of the *o*-substituted imidazole moiety or to coupled vibrations from both the imidazole and phenolate groups.[9] We also observed a positive band at 1548 cm^{-1} in the photolysis spectrum of our model His−phenol compound, which was not observed in the FT-IR difference spectrum of tyrosine (Figure 9). However, a positive band at the same frequency was also observed in the photolysis spectrum of the His−Tyr dipeptide, raising questions about the assignment of this band to the His−Tyr cross-link.

Copper-Containing Model Compounds. While our studies[9] and those of others[83,84] indicate that the cross-link causes only a slight perturbation in the EPR spectra of the cross-linked radical compared to an unmodified tyrosyl radical, the situation may be different for a His-phenol cross-link incorporated into a Cu-containing ligand framework. How the pK_a of such a compound would be affected is unknown. A very limited number of copper-containing model complexes incorporating the histidine−tyrosine cross-link have been synthesized and characterized.[40] He et al.[94] recently synthesized such a framework using tri(pyridylmethyl)amine ligands, in which one of the "legs" has a hydroquinone or a quinone substituent. Two-electron oxidation of the square planar complex [Cu(k^3N−H_2L^2)Cl_2] was associated with the loss of two protons and a conformational change, involving the binding of the hydro-

quinone substituent to the copper. This complex provides an example of a redox-driven and proton-linked conformational change, a key step in a proposed proton pumping mechanism of heme−copper oxidases. Karlin and co-workers recently prepared Cu(I) and Cu(II) complexes incorporating an imidazole−phenol cross-link.[95] The complexes contained either a tetradentate or tridentate pyridylalkylamine-containing chelate and their X-ray structures were reported. Both the tridentate and the tetradentate chelate Cu(I) complexes formed peroxodicopper(II) intermediates upon reaction with dioxygen at low temperatures. The formation of phenoxyl radical was not observed. Collman and co-workers have reported the synthesis of a model of cytochrome oxidase containing a proximal imidazole tail and three distant imidazoles attached to a porphyrin, one of which is cross-linked to a phenol.[96] Liu et al.[97] recently reported the first example of the synthesis and spectroscopic characterization of a heme−Cu complex possessing a cross-linked tyrosine−histidine mimic. A stable, low-temperature Fe(II) and Cu(I) peroxo product was formed upon reaction of the complex with dioxygen. We are currently investigating the cross-linked His−phenol incorporated into a Cu-containing ligand network. Preliminary studies indicate that the pK_a of the phenolic proton is also significantly lower than that observed for unperturbed tyrosine.

Summary and Perspectives. Our studies and those of others suggest that the cross-linked tyrosine in heme−copper oxidases may facilitate the cleavage of the dioxygen bond by functioning as a proton and an electron donor, thus generating a tyrosyl radical. The cross-linked tyrosine may also act as a proton donor during other steps in the enzyme's catalytic cycle. The optical spectral properties, both the time-resolved optical absorption difference spectra and the FT-IR difference spectra, of the photoinduced His−phenol model radical were significantly different from that of unperturbed tyrosinate. These differences could arise from the small delocalization of spin density onto the imidazole in the cross-linked compound. Further spectroscopic studies on Cu−His−phenol cross-link models and their UV-generated radical are in progress and are expected to provide an important insight into the structural and functional role of the histidine−tyrosine cross-link in heme−copper oxidases.

Acknowledgment. Supported by GM43273 (B.A.B.) and GM53788 (Ó.E.).

References and Notes

(1) Smith, W. L.; Eling, T. E.; Kulmacz, R. J.; Marnett, L. J.; Tsai, A.-L. *Biochemistry* **1992**, *31*, 3−7.
(2) Larsson, A.; Sjoberg, B.-M. *EMBO J.* **1986**, *5*, 2037−2040.
(3) Barry, B. A.; Babcock, G. T. *Proc. Natl. Acad. Sci. U.S.A.* **1987**, *84*, 7099−7103.
(4) Marcus, R. A. *Pure Appl. Chem.* **1997**, *69*, 13−29.
(5) Ostermeier, C.; Harrenga, A.; Ermler, U.; Michel, H. *Proc. Nat. Acad. Sci. U.S.A.* **1997**, *94*, 10547−10553.
(6) Yoshikawa, S.; Shinzawa-Itoh, K.; Nakashima, R.; Yaono, R.; Yamashita, E.; Inoue, N.; Yao, M.; Fei, M. J.; Libeu, C. P.; Mizushima, T.; Yamaguchi, H.; Tomizaki, T.; Tsukihara, T. *Science* **1998**, *280*, 1723−1729.
(7) Whittaker, M. M.; Whittaker, J. W. *J. Biol. Chem.* **1990**, *265*, 9610−9613.
(8) Barry, B. A.; El-Deeb, M. K.; Sandusky, P. O.; Babcock, G. T. *J. Biol. Chem.* **1990**, *265*, 20139−20143.
(9) Cappuccio, J. A.; Ayala, I.; Elliott, G.; Szundi, I.; Lewis, J.; Konopelski, J. P.; Barry, B. A.; Einarsdóttir, Ó. *J. Am. Chem. Soc.* **2002**, *124*, 1750−1760.
(10) Land, E. J.; Porter, G.; Strachan, E. *Trans. Faraday Soc.* **1961**, *57*, 1885−1893.
(11) Dixon, W. T.; Murphy, D. *J. Chem. Soc., Faraday Trans. 2* **1976**, *72*, 1221−1229.
(12) Harriman, A. *J. Phys. Chem.* **1987**, *91*, 6102−6104.
(13) Jovanovic, S. V.; Harriman, A.; Simic, M. G. *J. Phys. Chem.* **1986**, *90*, 1935−1939.
(14) Box, H. C.; Budzinski, E. E.; Freund, H. G. *J. Phys. Chem.* **1974**, *61*, 2222−2226.
(15) Dixon, W. T.; Moghimi, M.; Murphy, D. *J. Chem. Soc., Faraday Trans. 2* **1974**, *70*, 1713−1720.
(16) Sealy, R. C.; Harman, L.; West, P. R.; Mason, R. P. *J. Am. Chem. Soc.* **1985**, *107*, 3401−3406.
(17) Hulsebosch, R. J.; Van der Brink, J. S.; Niewenhuis, A. M.; Gast, P.; Raap, J.; Lugtenburg, J.; Hoff, A. J. *J. Am. Chem. Soc.* **1997**, *119*, 8685−8694.
(18) Nwobi, O.; Higgins, J.; Xuefeng, Z.; Ruifeng, L. *Chem. Phys. Lett.* **1997**, *272*, 155−161.
(19) Wise, K. E.; Pate, J. B.; Wheeler, R. A. *J. Phys. Chem. B* **1999**, *103*, 4764−4772.
(20) Dole, F.; Diner, B. A.; Hoganson, C. W.; Babcock, G. T.; Britt, R. D. *J. Am. Chem. Soc.* **1997**, *119*, 11540−11541.
(21) Tripathi, G. N. R.; Schuler, R. H. *J. Chem. Phys.* **1984**, *81*, 113−121.
(22) Johnson, C. R.; Ludwig, M.; Asher, S. A. *J. Am. Chem. Soc.* **1986**, *108*, 905−912.
(23) Takeuchi, H.; Watanabe, N.; Satoh, Y.; Harada, I. *J. Raman Spectrosc.* **1989**, *20*, 233−237.
(24) Mukherjee, A.; McGlashen, M. L.; Spiro, T. G. *J. Phys. Chem.* **1995**, *99*, 4912−4917.
(25) Boerner, R. J.; Barry, B. A. *J. Biol. Chem.* **1993**, *268*, 17151−17154.
(26) Pujols-Ayala, I.; Barry, B. A. *Biochim. Biophys. Acta* **2004**, *1655*, 205−216.
(27) Silva, K. E.; Elgren, T. E.; Que, L., Jr.; Stankovich, M. T. *Biochemistry* **1995**, *34*, 14093−14103.
(28) Sahlin, M.; Sjoberg, B.-M. *Subcell. Biochem.* **2000**, *35*, 405−443.
(29) Gie, J.; Yu, G.; Ator, M.; Stubbe, J. *Biochemistry* **2003**, *42*, 10071−10083.
(30) Kolaskar, A. S.; Sawant, S. *Int. J. Pept. Protein Res.* **1996**, *47*, 110−116.
(31) Kocak, A.; Luque, R.; Diem, M. *Biopolymers* **1998**, *46*, 455−463.
(32) Walden, S. E.; Wheeler, R. A. *J. Am. Chem. Soc.* **1997**, *119*, 3175−3176.
(33) Ayala, I.; Range, K.; York, D.; Barry, B. A. *J. Am. Chem. Soc.* **2002**, *124*, 5496−5505.
(34) Krimm, S.; Bandekar, J. *Adv. Protein Chem.* **1986**, *38*, 181−364.
(35) Manas, E. S.; Getahun, Z.; Wright, W. W.; DeGrado, W. F.; Vanderkooi, J. M. *J. Am. Chem. Soc.* **2000**, *122*.
(36) Haris, P. I.; Chapman, D. *Biopolymers* **1995**, *37*, 251−263.
(37) Okeley, N. M.; van der Donk, W. A. *Chem. Biol.* **2000**, *7*, R159−R171.
(38) Ito, N.; Phillips, S. E. V.; Stevens, C.; Ogel, Z. B.; McPherson, M. J.; Keen, J. N.; Yadav, K. D. S.; Knowles, P. F. *Nature* **1991**, *350*, 87−90.
(39) Rogers, M. S.; Dooley, D. M. *Curr. Op. Chem. Biol.* **2003**, *7*, 189−196.
(40) Kim, E.; Chufán, E. E.; Kamaraj, K.; Karlin, K. D. *Chem. Rev.* **2004**, *104*, 1077−1133.
(41) Stubbe, J.; van der Donk, W. A. *Chem. Rev.* **1998**, *98*, 705−762.
(42) Babcock, G. T.; Wikström, M. *Nature* **1992**, *356*, 301−309.
(43) Ferguson-Miller, S.; Babcock, G. T. *Chem. Rev.* **1996**, *96*, 2889−2907.
(44) Zaslavsky, D.; Gennis, R. B. *Biochim. Biophys. Acta* **2000**, *1458*, 164−179.
(45) Brzezinski, P.; Larsson, G. *Biochim. Biophys. Acta* **2003**, *1605*, 1−13.
(46) Wikström, M. *Nature* **1977**, *266*, 271−273.
(47) Iwata, S.; Ostermeier, C.; Ludwig, B.; Michel, H. *Nature* **1995**, *376*, 660−669.
(48) Tsukihara, T.; Aoyama, H.; Yamashita, E.; Tomizaki, T.; Yamaguchi, H.; Shinzawa-Itoh, K.; Nakashima, R.; Yaono, R.; Yoshikawa, S. *Science* **1996**, *272*, 1136−1144.
(49) Konstantinov, A. A.; Siletsky, S.; Mitchell, D.; Kaulen, A.; Gennis, R. B. *Proc. Natl. Acad. Sci. U.S.A.* **1997**, *94*, 9085−9090.
(50) Ädelroth, P.; Ek, M. S.; Mitchell, D. M.; Gennis, R. B.; Brzezinski, P. *Biochemistry* **1997**, *36*, 13824−13829.
(51) Verkhovskaya, M. L.; Garcia-Horsman, A.; Puustinen, A.; Rigaud, J. L.; Morgan, J. E.; Verkhovsky, M. I.; Wikström, M. *Proc. Nat. Acad. Sci. U.S.A.* **1997**, *94*, 10128−10131.
(52) Brzezinski, P.; Ädelroth, P. *J. Bioenerg. Biomembr.* **1998**, *30*, 99−107.
(53) Watmough, N. J.; Katsonouri, A.; Little, R. H.; Osborne, J. P.; Furlong-Nickels, E.; Gennis, R. B.; Brittain, T.; Greenwood, C. *Biochemistry* **1997**, *36*, 13736−13742.
(54) Gennis, R. B. *Biochim. Biophys. Acta* **1998**, *1365*, 241−248.
(55) Jünemann, S.; Meunier, B.; Gennis, R. B.; Rich, P. R. *Biochemistry* **1997**, *36*, 14456−14464.
(56) Ädelroth, P.; Gennis, R. B.; Brzezinski, P. *Biochemistry* **1998**, *37*, 2470−2476.
(57) Zaslavsky, D.; Gennis, R. B. *Biochemistry* **1998**, *37*, 3062−3067.

(58) Ruitenberg, M.; Kannt, A.; Bamberg, E.; Ludwig, B.; Michel, H.; Fendler, K. *Proc. Natl. Acad. Sci. U.S.A.* **2000**, *97*, 4632−4636.
(59) Wikström, M.; Jasaitis, A.; Backgren, C.; Puustinen, A.; Verkhovsky, M. *Biochim. Biophys. Acta* **2000**, *1459*, 514−520.
(60) Bränden, M.; Sigurdson, H.; Namslauer, A.; Gennis, R. B.; Ädelroth, P.; Brzezinski, P. *Proc. Natl. Acad. Sci. U.S.A.* **2001**, *98*, 5013−5018.
(61) Soulimane, T.; Buse, G.; Bourenkov, G. P.; Bartunik, H. D.; Huber, R.; Than, M. E. *EMBO J.* **2000**, *19*, 1766−1776.
(62) Swensson-Ek, M.; Abramson, J.; Larsson, G.; Törnroth, S.; Brzezinski, P.; Iwata, S. *J. Mol. Biol.* **2002**, *321*, 329−339.
(63) Buse, G.; Soulimane, T.; Dewor, M.; Meyer, H. E.; Blüggel, M. *Protein Sci.* **1999**, *8*, 985−990.
(64) Das, T. K.; Pecoraro, C.; Tomson, F. L.; Gennis, R. B.; Rousseau, D. L. *Biochemistry* **1998**, *37*, 14471−14476.
(65) Pinakoulaki, E.; Pfitzner, U.; Ludwig, B.; Varotsis, C. *J. Biol. Chem.* **2002**, *277*, 13563−13568.
(66) Proshlyakov, D. A.; Pressler, M. A.; Babcock, G. T. *Proc. Natl. Acad. Sci. U.S.A.* **1998**, *95*, 8020−8025.
(67) Proshlyakov, D. A.; Pressler, M. A.; DeMaso, C.; Leykam, J. F.; DeWitt, D. L.; Babcock, G. T. *Science* **2000**, *290*, 1588−1591.
(68) Blomberg, M. R. A.; Siegbahn, P. E. M. *Inorg. Chem.* **2003**, *42*, 5231−5243.
(69) Siegbahn, P. E. M.; Blomberg, M. R. A. *Biochim. Biophys. Acta* **2004**, *1655*, 45−50.
(70) Chen, Y. R.; Sturgeon, B. E.; Gunther, M. R.; Mason, R. P. *J. Biol. Chem.* **1999**, *274*, 3308−3314.
(71) MacMillan, F.; Kannt, A.; Behr, J.; Prisner, T.; Michel, H. *Biochemistry* **1999**, *38*, 9179−9184.
(72) Uchida, T.; Mogi, T.; Kitagawa, T. *Biochemistry* **2000**, *39*, 6669−6678.
(73) Nyquist, R. M.; Heitbrink, D.; Bolwien, C.; Gennis, R. B.; Heberle, J. *Proc. Natl. Acad. Sci. U.S.A.* **2003**, *100*, 8715−8720.
(74) Proshlyakov, D. A. *Biochim. Biophys. Acta* **2004**, *1655*, 282−289.
(75) Elliott, G. I.; Konopelski, J. P. *Org. Lett.* **2000**, *2*, 3055−3057.
(76) McCauley, K. M.; Vrtis, J. M.; Dupont, J.; Van der Donk, W. A. *J. Am. Chem. Soc.* **2000**, *122*, 2403−2404.
(77) Collman, J. P.; Wang, Z.; Zhong, M.; Zeng, L. *J. Chem. Soc., Perkin Trans. 1* **2000**, *1*, 1217−1221.
(78) Himo, F.; Noodleman, L.; Blomberg, M. R. A.; Siegbahn, P. E. M. *J. Phys. Chem. A* **2002**, *106*, 8757−8761.
(79) Fabian, M.; Palmer, G. *Biochemistry* **1995**, *34*, 13802−13810.
(80) Rigby, S. E. J.; Jünemann, S.; Rich, P.; Heathcote, P. *Biochemistry* **2000**, *39*, 5921−5928.
(81) Svistunenko, D. A.; Wilson, M. T.; Cooper, C. E. *Biochim. Biopys. Acta* **2004**, *1655*, 372−280.
(82) Chen, Y.-R.; Gunther, M. R.; Mason, R. P. *J. Biol. Chem.* **1999**, *274*, 3308−3314.
(83) Himo, F.; Erikson, L. A.; Blomberg, M. R. A.; Siegbahn, P. E. M. *Int. J. Quantum Chem.* **2000**, *76*, 714−723.
(84) Kim, S. H.; Aznar, C.; Bynda, M.; Silks, L. A. P.; Michalczyk, R.; Unkefer, C. J.; Woodruff, W. H.; Britt, D. R. *J. Am. Chem. Soc.* **2004**, *126*, 2328−2338.
(85) Aki, M.; Ogura, T.; Naruta, Y.; Le, T. H.; Sato, T.; Kitagawa, T. *J. Phys. Chem. A* **2002**, *106*, 3436−3444.
(86) Gennis, R. B. *FEBS Lett.* **2003**, *555*, 2−7.
(87) Qin, Y.; Wheeler, R. A. *J. Chem. Phys.* **1995**, *102*, 1689−1698.
(88) Iwaki, M.; Breton, J.; Rich, P. R. *Biochim. Biophys. Acta* **2002**, *1555*, 116−121.
(89) Iwaki, M.; Puustinen, A.; Wiström, M.; Rich, P. R. *Biochemistry* **2003**, *42*, 8809−8817.
(90) Hellwig, P.; Pfitzner, U.; Behr, J.; Rost, B.; Pesavento, R. P.; van der Donk, W. A.; Gennis, R. B.; Michel, H.; Ludwig, B.; Mäntele, W. *Biochemistry* **2002**, *41*, 9116−9125.
(91) Venyaminov, S. Y.; Kalnin, N. N. *Biopolymers* **1990**, *30*, 1243−1257.
(92) McMahon, B. H.; Fabian, M.; Tomson, F.; Causgrove, T. P.; Bailey, J. A.; Rein, F. N.; Dyer, R. B.; Palmer, G.; Gennis, R. B.; Woodruff, W. H. *Biochim. Biophys. Acta* **2004**, *1655*, 321−331.
(93) Tomson, F.; Bailey, J. A.; Gennis, R. B.; Unkefer, C. J.; Zizhong, L.; Silks, L. A.; Martinez, R. A.; Donohoe, R. J.; Dyer, R. B.; Woodruff, W. H. *Biochemistry* **2002**, *41*, 14383−14390.
(94) He, A.; Colbran, S. B.; Craig, D. C. *Chem. Eur. J.* **2003**, *9*, 116−129.
(95) Kamaraj, K.; Kim, E.; Galliker, B.; Zakharov, L. N.; Rheingold, A. L.; Zuberbühler, A. D.; Karlin, K. D. *J. Am. Chem. Soc.* **2003**, *125*, 6028−6029.
(96) Collman, J. P.; Decréau, R. A.; Zhang, C. *J. Org. Chem.* **2004**, *69*, 3546−3549.
(97) Liu, J.-G.; Naruta, Y.; Tani, F.; Chishiro, T.; Tachi, Y. *Chem. Commun.* **2004**, 120−121.
(98) Budimann, K.; Kannt, A.; Lyubenova, S.; Richter, O.-M. H.; Ludwig, B.; Michel, H.; MacMillan, F. *Biochemistry* **2004**, *43*, 11709−11716.